Environmental Advances 11 (2023) 100332

Contents lists available at ScienceDirect

Environmental Advances

journal homepage: www.sciencedirect.com/journal/environmental-advances

Accumulation and transport of atmospherically deposited PFOA and PFOS in undisturbed soils downwind from a fluoropolymers factory

Thomas Gerardu [a,b], Joris Dijkstra [a], Henry Beeltje [c,d], Alex van Renesse van Duivenbode [c], Jasper Griffioen [a,e,*]

[a] TNO Geological Survey of the Netherlands, Utrecht, the Netherlands
[b] Tebodin, Enschede, the Netherlands
[c] TNO Environmental Modelling, Sensing & Analysis, Utrecht, the Netherlands
[d] Aquon, Tiel, the Netherlands
[e] Copernicus Institute of Sustainable Development, Utrecht University, Utrecht, the Netherlands

ARTICLE INFO

Keywords:
PFAS sorption
Sand
Peat
HYDRUS
The Netherlands

ABSTRACT

PFOA and PFOS are widely found PFAS components in Dutch topsoils. PFOA was emitted to the atmosphere during 1970-2012 from a fluoropolymers factory, and was deposited mainly within a radius of 50 km. For the first time, detailed concentration-depth profiles of PFOA and PFOS were measured in undisturbed soils downwind of the factory. Three locations were selected with about 3 meters of sand soil and free infiltration of rain. An adjacent peat soil was selected for comparison. In the sand soils, concentration-depth profiles of PFOA showed a distinct bell-shaped pattern with the highest contents at 0.2-0.5 m below surface, and lower contents both at the surface and at further depth (up to 3.5 m below surface). This observation indicates that the highest atmospheric deposition has passed, and that PFOA gradually migrates towards groundwater. Concentrations of PFOS are highest near the surface and reach the detection limit at 1 m below surface, suggesting that its downward migration occurs much slower. HYDRUS was used to model PFAS transport in the vadose zone assuming steady-state infiltration. The PFOA depth profiles in the sand soils can be described assuming plausible historic, atmospheric emission of PFOA from the factory and K_{oc} values within the literature range. However, the retention observed must be attributed to linear partitioning between water and both soil organic matter and the air-water interface. Somewhat stronger retention holds for PFOS, but PFOS cannot originate from the factory in the extent found. An alternative explanation is historic, rather parallel emissions from nearby sources such as waste incinerators. Based on measurements and modelling, this study illustrates that PFOA, and to a lesser extent PFOS, should not be treated as immobile contaminants in topsoil as is currently the case in Dutch soil policy, but rather as mobile contaminants of which the legacy amounts in soil will pollute groundwater for many decades.

Introduction

Poly- and perfluoro-alkyl substances (PFAS) are chemicals that have unique surface-active properties. They are both water and oil repellent and are highly resistant to heat and acids. These properties explain their widespread use in the industry and in consumer products (Glüge et al., 2020; Cordner et al., 2021). Since 2000, they have come under increasing environmental attention because these substances are persistent, bioaccumulative and toxic (Buck et al., 2011). PFAS contamination of soil, surface water and groundwater is widespread (e.g. Zareitalabad al. 2013, Joerss et al. 2019, Li et al. 2020, Ma et al. 2022). PFAS are a potential threat for drinking water (e.g. Eschauzier et al. 2013, Zafeiraki et al. 2015, Herrick et al. 2017) and a risk with respect to bio-accumulation and food quality (Ghisi et al., 2019; Schulz et al., 2020; Wang et al., 2020).

The past few years, awareness has further grown of the possibly negative health effects of (long-term) exposure to PFAS. Four EU countries from Northern Europe asked the European Commission to formulate actions to reduce emissions of PFAS to the environment (CEU, 2019a) after an earlier call by the European Council on the European Commission to develop an action plan to eliminate all non-essential uses of PFAS (CEU, 2019b). More recently, the European Food Safety

* Corresponding author at: Copernicus Insititute of Sustainable Development, Utrecht University, Utrecht, the Netherlands.
E-mail address: j.griffioen@uu.nl (J. Griffioen).

https://doi.org/10.1016/j.envadv.2022.100332

Available online 10 December 2022

Authority (EFSA) recommended a lowering of the standard for tolerable weekly intake via food (EFSA, 2020). This also necessitated the Dutch National Institute for Public Health and Environment (RIVM) to recommend a lower limit for drinking water as the human intake of PFAS is largely determined by drinking water use and food consumption (RIVM, 2021). Not only insight in the presence of PFAS in the environment is thus important but also in their behaviour in order to understand their fate and the environmental and health risks both at present and in the future.

PFAS are composed of a fluorinated carbon chain with a functional group, and usually well soluble in water. Their environmental behaviour may be complex as they show both hydrophylic and hydrophobic properties. Basically, they show partitioning behaviour between water and organic matter due to their hydrophobic properties, ion exchange behaviour as dissociated acid to oppositely (and pH-dependent) charged sites of the soil matrix and electrostatic interaction due to the high electronegativity of the fluorine atom (Du et al., 2014; Zhang et al., 2019). These interaction processes also imply that they not only sorb to organic matter but also to minerals especially oxides and clay minerals (Zhang et al., 2019). Their properties as surfactant imply that they may show air-water interfacial adsorption as additional retention mechanism in unsaturated soils (Guo et al., 2020; Silva et al., 2020). They also show lipophobic behaviour which makes them both water and fat repellent. Additionally, the presence of organic immiscible liquids (NAPLs) further complicates the fate of PFAS in the environment as they may accumulate at the water-NAPL interface and partition to NAPLs (Brusseau, 2018).

The recognition of widespread contamination of soil and groundwater with PFAS also induces a need how to consider PFAS contamination from a legislative perspective. This especially holds for the Netherlands being a heavily industrialised and densely populated country, where soil and groundwater are also strongly impacted by anthropogenic contamination. In recent years, awareness has grown that there is considerable diffuse contamination of especially PFOA and PFOS across the Netherlands in addition to local, point-source contamination at sites where, for example, fire drills were executed. Diffuse contamination is in the southwestern part of the Netherlands strongly attributed to the atmospheric emission of PFAS from a factory in Dordrecht (Western Netherlands; RIVM, 2020; Brandsma et al., 2019; Gebbink and Van Leeuwen, 2020). The factory used PFOA for the production of, among other, Teflon® and Viton® between 1970 and 2012 (Koch et al., 2017; Zeilmaker et al., 2016), after which PFOA was replaced by GenX, a substitute chemical with similar properties and behaviour. PFOA has also been released from the factory in surface waters as effluent (Rijkswaterstaat 2017a; Expertisecentrum PFAS, 2018b). The most severe topsoil contamination with PFOA has been found within a 50 km radius of the factory in Dordrecht (RIVM, 2020).

The earlier awareness of widespread soil contamination with both PFOA and PFOS had set the need for national background values, in addition to a value that reflects zero or negligible contamination. For the latter, a generic value of 0.1 μg/kg is used in the Netherlands. The background values are established to prevent the further spreading of PFAS-contaminated soil, and reflect the contamination level of PFAS that can be assumed to be already present in the soil throughout the Netherlands (RIVM, 2020). If the PFAS concentration in a soil is lower than the background value, that soil may be moved elsewhere according to rules of the Soil Quality Decree (e.g., for application in infrastructural works). In July 2020, the compound-specific background values were set to 1.9 and 1.4 μg/kg for PFOA and PFOS, respectively (note the ratio of 1.4 for later), for the Netherlands as based on systematic, national monitoring (RIVM, 2020). Elevated levels in the 50 km zone around the factory were excluded when deriving the background levels.

It is unknown how PFOA, originating from the factory and transported through the atmosphere, behaves in soil, as governed by the historical PFOA atmospheric deposition, rainfall, and hydrological and chemical soil properties. It is also unknown how PFOS compares to PFOA, where the first was not processed at the factory but is found to be omnipresent in Dutch soils, and hence must originate from other diffuse sources such as waste incinerators (Expertisecentrum PFAS, 2017, 2018a). Such insights are needed to evaluate how soil and groundwater contamination relate to each other (Newell et al., 2021).

This research aims to understand PFOA and PFOS contamination in soils, as a result of decades of atmospheric deposition in the vicinity of a fluoropolymers factory. We investigate the extent to which these substances have migrated towards larger depth, and whether a content-depth pattern is observed that can be related to estimates of the historic emission from the factory. To this end, detailed content-depth profiles of PFOA and PFOS were collected in undisturbed soil profiles and interpreted with a 1D reactive transport model, with the purpose to explain observed content profiles as a function of soil properties, substance properties, and historic atmospheric deposition.

Materials and methods

Historic PFOA and PFOS emissions

The fluoropolymers factory (51°49′3.37"N, 4°43′42.18"E) is located in the harbour area of the city of Dordrecht, The Netherlands. The production of Teflon® and other fluoropolymers containing products started at the factory in 1970. According to Zeilmaker et al. (2016) PFOA was used as dispersant in the polymer preparation of Teflon®, FEP and Viton® until 2012 after which GenX was used for this purpose. During production, PFOA is released as a gas during a drying process. The gaseous PFOA coagulates upon release and forms aerosols of which 10% is of the size 1-2.5 μm and 90% is 0-1 μm. Based on information from permits and from the factory itself, estimates for the PFOA emissions to the atmosphere are between 1600 and 6800 kg y^{-1} (1985-2002), followed by lower emissions of 100-500 kg y^{-1} (2003-2012, Zeilmaker et al., 2016; Koch et al., 2017; see also Table 1).

PFOA containing waste water was also directly discharged into the river until to 2000. Since 2000, the waste water from the production process has discharged to a municipal waste water treatment installation (MWWT) with some other waste waters from the factory but incidental discharges directly to the river did occur. In 2017, the mixed influent from the factory plant to the MWWT contained 1000s ng PFOA/L and irregular concentrations of PFOS from mostly below detection limit up to 1500 ng/L (Rijkswaterstaat, 2017a). The effluent of the MWWT contained 100s ng PFOA/L and 10-20 ng PFOS/L. Additional waste water streams that discharge directly to the river are also present among which one from the groundwater treatment facility associated with the on-going groundwater remediation project at the factory plant (Rijkswaterstaat, 2017a). The effluent of this facility contained in 2017 1000s ng PFOA/L and 10s ng PFOS/L. The other waste water streams contain up to 100s ng PFOA/L and up to 10s ng PFOS/L. Outside GenX, five out of 11 other PFAS compounds were frequently detected in the waste waters at levels slightly higher than PFOS, four at intermediate to low level and 2 were not detected at all. All these data illustrate that the concentration levels of PFOA at the factory plant are considerably higher than those of PFOS and other PFAS compounds. This is also supposed to

Table 1
Overview of sampling locations (coordinates known to the authors and available on request) and the samples taken for laboratory analysis.

Code	Location	Number of samples	Sampling depths (cm-bs)
Sand 1	Schoonenburgsche Heuvel	12	10, 20, 30, 40, 50, 60, 70, 100, 150, 220, 300, 350
Peat	At the foot of Schoonenburgsche Heuvel	8	10, 30, 50, 70, 90, 110, 130, 140
Sand 2	De Donk	8	10, 20, 40, 60, 80, 120, 200, 300
Sand 3	Hoornaar	12	5, 10, 20, 30, 40 50, 60, 70, 100, 150, 200, 250.

be the situation before 2017. It points out that PFOA is the PFAS compound associated with the factory that is of most environmental concern (outside GenX; Brandsma et al., 2019; Gebbink and Van Leeuwen, 2020).

Sampling locations

Two earlier monitoring campaigns investigated the PFAS contamination status within 20 km from the factory (Expertisecentrum PFAS, 2017; 2018a). 33 sites were sampled that were supposed to be undisturbed in the past 20 years and not suspected of local PFAS contamination. The results indicate that the median PFOA content was 5.1 and 5.0 μg/kg soil for a soil layer of 0-20 and 20-50 cm below surface (henceforth referred to as cm-bs), respectively. The median PFOS content was 0.76 and 0.20 μg/kg for a soil layer of 0-20 and 20-50 cm-bs, respectively. Eight other PFAS compounds were also regularly detected but less frequent and at levels lower than PFOA and PFOS; 11 other PFAS compounds were not detected at all.

For the soil sampling in the present study, a series of requirements was formulated in order to couple the depth profiles of PFOA with the deposition history and associated emission history from the factory: 1. in predominantly N-NE direction from the factory considering that the wind direction is almost 50% of the time West to South in the Western Netherlands, 2. vertical infiltration of precipitation and absence of seepage, 3. homogeneous soil, either sand or peat, 4. not disturbed, i.e., no tillage in the past 50 years and 5. rural area so other sources of PFAS do not play a role. Based on these criteria, inland dunes that are present in the riverine part of the Central Netherlands were the preferred locations. These dunes are composed of aeolian sand and occur as local outcrops in the flat polder landscape of the Central and Western Netherlands. They have an altitude several meters above their surroundings, which causes the groundwater level to be relatively deep and infiltration of rain water is typically vertical. They are called 'donk' in Dutch so the name of one of the sampling sites directly refers to the geomorphological feature. Three sites with sand soils were identified using Google Earth, digital elevation data, historical topographic maps and geological data (Fig. 1). A fourth site with peat soil (referred to as Peat) and adjacent to one of the sandy sites was also selected. This served to intercompare the total amount of deposited PFAS where the peat soil was assumed to have a high sorption capacity and the sand soils a low one. An exploratory visit was made to the locations to ask for permission as all locations are on private land and to check the conditions.

Field sampling procedure

Precautions were taken to prevent possible sample contamination, largely following a national guideline on sampling PFAS contaminated soil (Expertisecentrum PFAS, 2020). Polyethylene sample containers that were pre-cleaned with methanol were used for collection of the soil samples, and any possible fluoropolymer- bearing equipment such as specific clothing was avoided.

An Edelman hand auger (Ø 7 cm) was used for drilling. Samples were taken with a stainless steel apple corer (pre-cleaned with methanol), and stored in 50 ml polyethylene sample jars. Soil samples of about 20 g each were collected from soil material drilled from every depth interval (Table 1). Sampling started at the deepest interval, to exclude any possibility of sample contamination of clean soil by presumably more contaminated shallow soil material. In parallel, soil samples were taken for thermogravimetric (TGA), CS-elemental and grain size analysis. At the three sand soils, the upper 100 cm were sampled with a higher resolution (every 10-20 cm) followed by a lower resolution (every 50-100 cm) down to 250-350 cm-bs. These depths were above the groundwater table, as found during the field work in October. This was done because exact groundwater levels and their temporal fluctuations were unknown and most variation in PFAS content was expected in the upper 100 cm. At the Peat location, samples were taken at regular intervals of 20 cm down to a depth of 140 cm which was below the groundwater table (50 cm-bs).

Sample pre-treatment and chemical analysis of PFOS and PFOA

The soil samples were analysed for the content of 18 PFAS substances among which PFOA and PFOS (see Supporting Information). Sample pretreatment and analysis followed the in-house protocol for PFAS analysis in soil samples. All laboratory equipment, tubing and

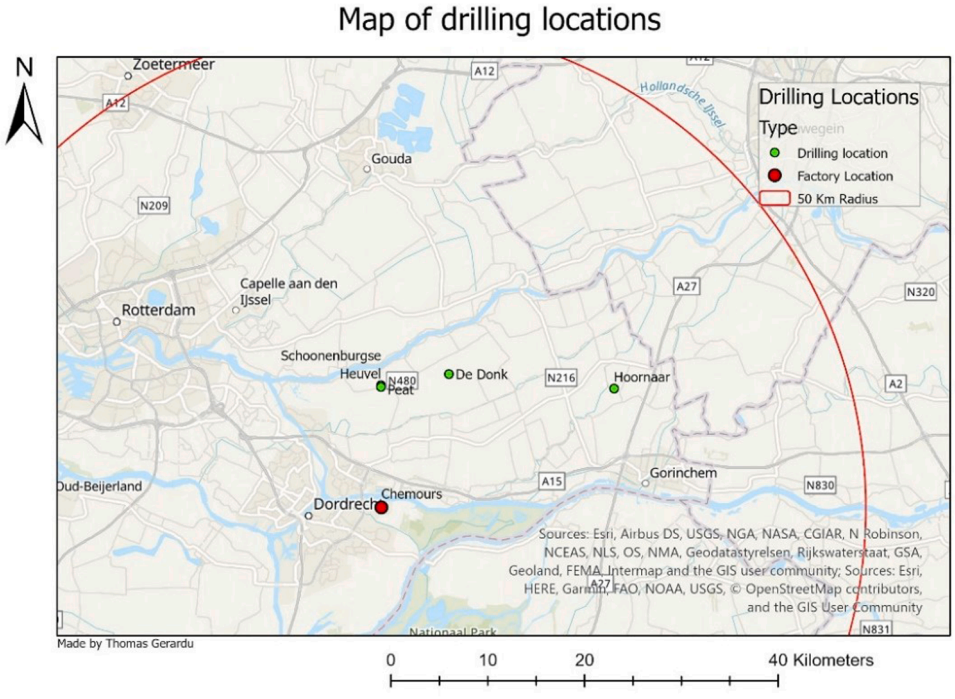

Fig. 1. Topographic map presenting the sampling sites and the location of the fluoropolymers factory.

disposables were fluoropolymer-free and tested for suitability for PFAS analysis. Parts of the LC-MSMS (Agilent) were replaced according to Application Note 5991-7863EN (Agilent Technologies, 2017), see Supporting Information. Glassware was avoided in order to prevent PFAS losses due to adsorption (Expertisecentrum PFAS, 2020 – see also below). Polypropylene (PP) or polyethylene (PE) vials, bottles, centrifuge tubes, tubing of the LC-MSMS were flushed with methanol before sample pre-treatment and analysis.

Before further processing, the field-moist soil samples were spiked with an internal standard consisting of certified mass-labeled perfluoroalkylcarboxylic acids and perfluoroalkylsulfonates (Wellington MPFAC-MXA). Next, the samples were dried for 48 h at 105°C, after which 2 grams was transferred to 15 ml pre-cleaned PP vials. First an extraction with 6 ml 2% formic acid in MilliQ was performed and subsequently twice an extraction with 2 ml methanol/milliQ (in 1:1 ratio) in order to extract as much PFAS molecules as possible. The extracts were applied on a conditioned SPE column (Waters Oasis WAX 3cc, 60 mg; conditioning: 2 ml 1% ammonia in methanol; 2 ml methanol; 2 ml 2% formic acid in MilliQ water) to concentrate the PFAS molecules on the sorption medium. The vials were additionally washed twice with 1.5 ml milliQ and once with 1.5 ml methanol, which were subsequently transferred to the SPE column. After this, the SPE columns were dried for 15 min at the maximum obtainable vacuum. Next, the columns were eluted in steps of 1 ml to a total of 3 ml of 1% ammonia in methanol and the elution was dried under nitrogen gas flow at c. 40°C. Finally, a 1:1 mixture of methanol and MilliQ was added to the dried extract in the vial to dissolve all the concentrated extract which was then inserted in 0.3 ml insert vials that were subsequently analysed with LC-MS (Agilent Technologies).

The amounts of PFAS in the samples were quantified based on the measured signal, the calibration lines and the recoveries of the mass-labeled substances in the soil samples. More details are provided in the Supporting Information on the analytical method, instrument settings and performance (recoveries, reproducibility and uncertainties) according to NEN 7779 (NEN - Netherlands Committee for Standardization, 2018) based on the mass-labeled substances. LOD and LOQ for PFOA and PFOS of this method were established at 0.1 and 0.3 μg/kg dry soil, respectively. Repeatability was checked for two samples in quadruple (Sand 1, 100 cm-bs; Sand 2, 120 cm-bs) for which the average and standard deviation of PFOA were 0.36 ± 0.09 and 0.93 ± 0.32 μg/kg, respectively. No PFAS was detectable in blanks that followed the full pre-treatment and analysis procedure. Additional indications that systematic sample contamination is unlikely is the observation that the deepest soil samples contained the lowest contents of PFOS and PFOA, of which PFOS was below detection limit at all locations, and PFOA below detection limit in the peat soil at 140 cm-bs. Recent work by Lath et al. (2019) and Zenobio et al. (2022) indicate that PFAS may adsorb to PP or PE material to a higher extent than to glassware, potentially leading to lower recoveries. As analytical results were corrected with recoveries of mass-labeled PFAS substances that followed the full method of pre-treatment and analysis and recoveries varied to a limited extent per compound, we do not expect the use of PE/PP to have significantly biased our results.

Determination of bulk soil parameters

Soil organic matter content was determined by both thermographic analysis (TGA) as organic matter (OM) and by CS elemental analyser as organic carbon (OC). Most soil samples are non-calcareous and a few low in Ca carbonate so we preferred not to remove carbonates prior to CS elemental analysis as this may also disturb the OC content to some extent. The combined results were used to calculate the sorption parameter K_d from K_{oc} (see later). OM is related to OC by a conversion factor, which was determined for the data set from a linear trend line.

During TGA analysis, the temperature increased gradually from 25°C to 1000°C over a pre-set time. Samples were first heated from 25°C to 105°C to evaporate all residual moisture from the initial soil sample after which the temperature stabilized for 3.5 h. Then the temperature was linearly increased from 105°C to 1000°C for 15 (± 1) h. In TGA, the weight losses between certain temperature intervals can be assigned to the loss of a certain soil compound, such as organic matter. The range 110-450°C is the typical temperature range where organic matter gets oxidised and lost. The mass loss in the range 450-550°C may be attributed to more recalcitrant soil organic matter, ferrous carbonate or dehydration of clay minerals (Roskam et al., 2008). Calcium carbonate starts to decompose above 600°C up to about 800°C (Kasozi et al., 2009; Roskam et al., 2008). The range 550-700°C may also be governed by mass loss from montmorillonite and pyrite. The Leco SC-632 was used for CS elemental analysis, which has a detection limit of 0.1% for carbon and 0.039% for sulphur. The measuring accuracy is 0.039% for carbon and 0.013% for sulphur. The results regarding the sulphur analysis did not have to be used.

Grain size distribution was determined using a Malvern Mastersizer. The samples were inserted in the instrument in a compartment of demineralised water. The analyses were used to determine texture classes based on the U.S. Department of Agronomy classification system (e.g. USDA 1987).

Reactive transport modelling approach

The model code HYDRUS (Šimůnek et al., 2008) was used to model reactive transport of PFAS in the unsaturated (or saturated) zone (version 4.17.0140). The four locations were assumed to have been exposed to PFAS deposition between 1970 and 2012 (assumed deposition rates see below), the models runs proceeded until at least 2020. The modelled content-depth profiles for 2020 were compared with the field data as collected in October 2020. The next paragraphs describe the parametrisation and pre-processing steps in detail.

The input parameters and parameterization for the soil properties are listed in Table 2. 'Default' reflects the standard parameter set in HYDRUS for soil texture classes and is based on Van Genuchten (1980), Carsel and Parrish (1988) and Schaap et al. (2001). The depth of the soil profiles was taken as the distance from surface to the water table at each location. The values for K_s, ρ, K_d were based on the results of the soil analyses. The bulk density (ρ) was derived from the texture class (De Vries, 1999) that was determined using the d50 value (grain size analysis). The K_s was set to 700 cm/d and based on Carsel and Parrish (1988) for medium sized sand.

In the absence of non-aqueous phase liquids, retention of PFAS in the unsaturated zone has been attributed to sorption to organic matter, clay

Table 2
Model parameters employed and parameterization. Length units are abbreviated as L, time as T, mass as M and volume as V.

Parameter	Symbol	Unit	Source
Depth of soil profile	-	L	Borehole data
Residual soil water content	θ_r	Fraction	Default
Saturated soil water content	θ_s	Fraction	Literature
Parameter *a* in the soil water retention function	-	L	Default
Parameter *n* in the soil water retention function	-	-	Default
Saturated hydraulic conductivity	K_s	L/T	Literature
Tortuosity parameter in the conductivity function	T	-	Default
Bulk density	ρ	M/V	Analysis + Literature
Dispersion Coefficient	D_L	L	Default
Fraction of adsorption	-	Fraction	Default
Molecular diffusion coefficient in free water	D_w	L^2/T	Literature
Adsorption coefficient	K_d	L^3/M	Analysis + Literature
Solute concentration of inflowing water	-	M/V	PFAS profiles

and silt, and oxides of in particular Fe as well as adsorption at the air-water interface (AWI). Sorption to these solids may be described with linear, Langmuir, Freundlich or other isotherms where the control by non-linear sorption increases with increasing maximum concentration considered and the sorption to the individual constituents has been assumed as additive (Milinovic et al., 2015; Nguyen et al., 2020; Zhou et al., 2021; Zeng and Guo, 2021). Adsorption at the AWI has been modelled as a Langmuir isotherm (e.g. Silva et al. 2020):

$$\Gamma^{PFAS} = \Gamma^{PFAS}_{max} \frac{K^{PFAS}_{ai}.c^{PFAS}}{1 + K^{PFAS}_{ai}.c^{PFAS}} \quad (1)$$

Where PFAS refers to a specific PFAS compound, Γ^{PFAS} is the adsorbed amount of that compound, Γ^{PFAS}_{max} is the associated maximum sorption capacity, c^{PFAS} is the aqueous concentration and K^{PFAS}_{ai} is the partitioning coefficient between the AIW and water.

Based on earlier investigation, we expect PFOA and PFOS contents up to 1-10 μg/kg (Expertisecentrum PFAS, 2017, 2018a). The associated pore water concentrations will be up to several hundreds ng/L (which is up to ~ 1 nmol/L). This is far below the solubilities of PFOA and PFOS in water being 9500 mg/L and 680 mg/L, respectively (EPA, 2017). The values for Γ^{PFOA}_{max} and Γ^{PFOS}_{max} are 4.5 × 10^{-6} and 5.1 × 10^{-6} mol/m^2, respectively, and those for K^{PFOA}_{ai} and K^{PFOS}_{ai} are 360 and 1970 L/mol, respectively (Vecitis et al., 2008). This means for PFOA or PFOS concentrations up to ~ 1 nmol/L that adsorption to the AWI is linear as the occupancy of the interface is far from saturated. It also means that the concentrations are too low: 1. to initiate surface tension reduction that causes changes in capillary pressure gradients and 2. to induce intermolecular interactions at the air-water interface between PFOA and PFOS (and other PFAS that may be present). Silva et al. (2020) indicated that solution concentrations in excess of 10 mg/L are generally needed before the effects of surface tension on unsaturated flow would be noticeably contributive. Concentrations above 1 mg/L are needed to make intermolecular interactions at the AWI become relevant (Silva et al., 2021). Thus, the presence of PFAS will not influence the soil physical conditions.

Taking into account the low concentrations expected, we assumed that all potential retention processes may be modelled as linear sorption and additive (Milinovic et al., 2015; Nguyen et al., 2020; Silva et al., 2020; Zhou et al., 2021; Zeng and Guo, 2021). For reference, we based the estimate of the sorption coefficient on the common equation for partitioning to soil organic matter:

$$S = K_d.C \quad (2)$$

and

$$K_d = K_{OC}.foc \quad (3)$$

where K_d is the sorption coefficient [L/kg], K_{oc} is the normalised organic carbon to water partition coefficient [L/kg] as collected from literature (Table 3), f_{oc} is the organic carbon content as fraction of the sample [g_{oc}/$g_{dry\ soil}$], S is the sorbed content [ng/kg wet soil] and C is the pore water concentration [ng/L]. The values for f_{oc} were based on the TGA and CS elemental analyser results. First, OC and OM data from all samples were plotted in a single graph to check on mutual consistency and outliers. Next, the slope of the regression line between OC and OM was used to determine f_{oc} from the OM contents determined by TGA for all samples. Based on OC and OM analyses, the number of soil layers was specified per profile.

Table 3
Log K_{oc} values employed in the model runs for PFOA and PFOS based on Nguyen et al. (2020) for soils with a near-neutral pH.

Compound	low	middle	high
PFOA	1.80	2.30	2.80
PFOS	2.70	3.10	3.50

The single porosity 'van Genuchten-Mualem' model was selected for water flow conditions with no hysteresis. Hysteresis was assumed irrelevant as we considered average annual rain water recharge for several decades. The upper model boundary condition was an atmospheric boundary layer that allowed ponding with a depth of 2 cm. The lower boundary condition was a constant head (constant water table), implying continuous unsaturated conditions for the entire profiles and neglecting seasonal or multi-year groundwater table fluctuations. In reality, the groundwater table was below the end of the boreholes at the time of drilling for the sand profiles. The default time- and space weighing scheme were selected: Crank-Nicholson and Galerkin Finite Elements, respectively. Tortuosity was selected with the default Millington and Quirk module. Model calculations were made for PFOA and PFOS where equilibrium sorption was assumed. As K_d was not known for the soils at hand and K_{oc} varies for PFOA and PFOS according to literature, four model runs were performed: run 1 with low K_{oc} values for PFOA and PFOS as obtained from literature, run 2 with intermediate values, run 3 with high values and run 4 with adjusted values for the best fit. The log K_{oc} employed (Table 3) was based on mean values plus or minus one standard deviation as presented in an extensive study by Nguyen et al. (2020). The four different depth profiles were compared to the measured profiles per PFAS compound.

Daily precipitation/evaporation data were obtained from the climate database of the Dutch Royal Netherlands Meteorological Institute (KNMI) for the weather station at Cabauw which is within 8-15 km from the drilling locations. The variables used were 24 h sum of precipitation (in 0.1 mm) and reference crop evaporation (Makkink) (in 0.1 mm). Cabauw's data log starts from 1986 until now whereas input data was needed from 1970 onwards. Thus, the most average year, 1988 with 725 mm precipitation and 525 mm evaporation, was chosen and repeated 16 times to fill in the data gap of 1970-1986. Preliminary model runs indicated that daily or yearly precipitation data did not influence the model results; hence, yearly data was used as the model runs were much faster. All four locations had the same meteorological dataset for precipitation and evaporation.

The upper boundary condition in the model was a concentration flux boundary, which corresponds to a variable input concentration of PFAS in the inflowing precipitation, and the lower boundary was set as zero concentration gradient, which allows free drainage of PFAS away from the profile. For the first boundary condition, the PFAS concentration in the precipitation was determined based on the assumption that the total deposition of PFOA and PFOS on each location is the same as the total amount present in the depth profile. In other words, all PFAS deposited is contained in the soil profile sampled. Volatilisation of PFAS from the soil is thus assumed negligible which seems justified as PFAS generally have a low volatility and their dissociation in water causes their affinity with the water phase to be stronger than with air (Wang et al., 2011). Together, this makes PFOA and PFOS less volatile than expected based on their physical properties alone (Prevedouros et al., 2006). The depth-integrated PFOA and PFOS contents were calculated from the profiles. The yearly precipitation concentrations of PFOA (in ng/cm^3 water) were proportionally matched to estimates of the yearly atmospheric emission of PFOA (Table 4), while the total precipitated amounts matched the depth- integrated PFOA and PFOS contents at each location. It was assumed that the atmospheric emission and deposition of PFOS parallels that of PFOA, in the absence of known characteristics of diffuse PFOS sources. Recent analyses of two rain water samples indicate PFOS concentration below detection limit of 1 ng/L and PFOA concentration of 6.6 ng/L at Lelystad (~ 110 km away in most prominent downwind direction) and below detection limit of 1 ng/L at Krommenie (~ 90 km away in near-equal direction; Rijkswaterstaat, 2020). This confirms there is a negligible background concentration in Dutch rain, justifying that no atmospheric deposition of PFOS and PFOA takes place after 2012.

The model produces a variety of output files where the following

Table 4
Estimated atmospheric emission history of PFOA from the factory as based on Zeilmaker et al. (2016) and Koch et al. (2017) and the proportional concentration in the precipitation.

Period	Average emission (in kg/year)	Relative concentration in precipitation
1970-1985	2500	5X
1985-1998	5000	10X
1998-2003	2500	5X
2003-2012	500	X

were used: concentration-depth profiles, water content-depth profiles, cumulative solute flux profiles and mass balance information.

Results

Soil characteristics

The grain-size analyses indicate that the sand soil profiles 1-3 contain medium sand with median values of 300-400 μm along the entire depth. Seventeen shallow samples contain 1.3-6.1% clay and 3.0-13.6% silt; fourteen deeper samples did not contain clay and silt. The results of the TGA indicate that Sand 1 and Sand 2 have 4-6% OM down to 30-40 cm-bs, about 1-2% in the next depth range to 50-80 cm-bs and less than 0.4% further down. Sand 3 is somewhat different with an OM content decreasing from 4 to 1% with depth to 70 cm-bs and less than 0.4% at 100 cm and deeper. For these sand soils, TGA indicates that the mass loss in the range 450-1000°C is small with values between 0.2 and 0.6% and no peaks. Here, three Sand 2 samples from 40-80 cm-bs are exceptions with TGA peaks of 0.2 - 0.3% between 600 and 700°C, which may be attributed to Ca carbonate. For the rest, the fractions of carbonate and clay minerals in the samples are very small. The fourth soil sampled

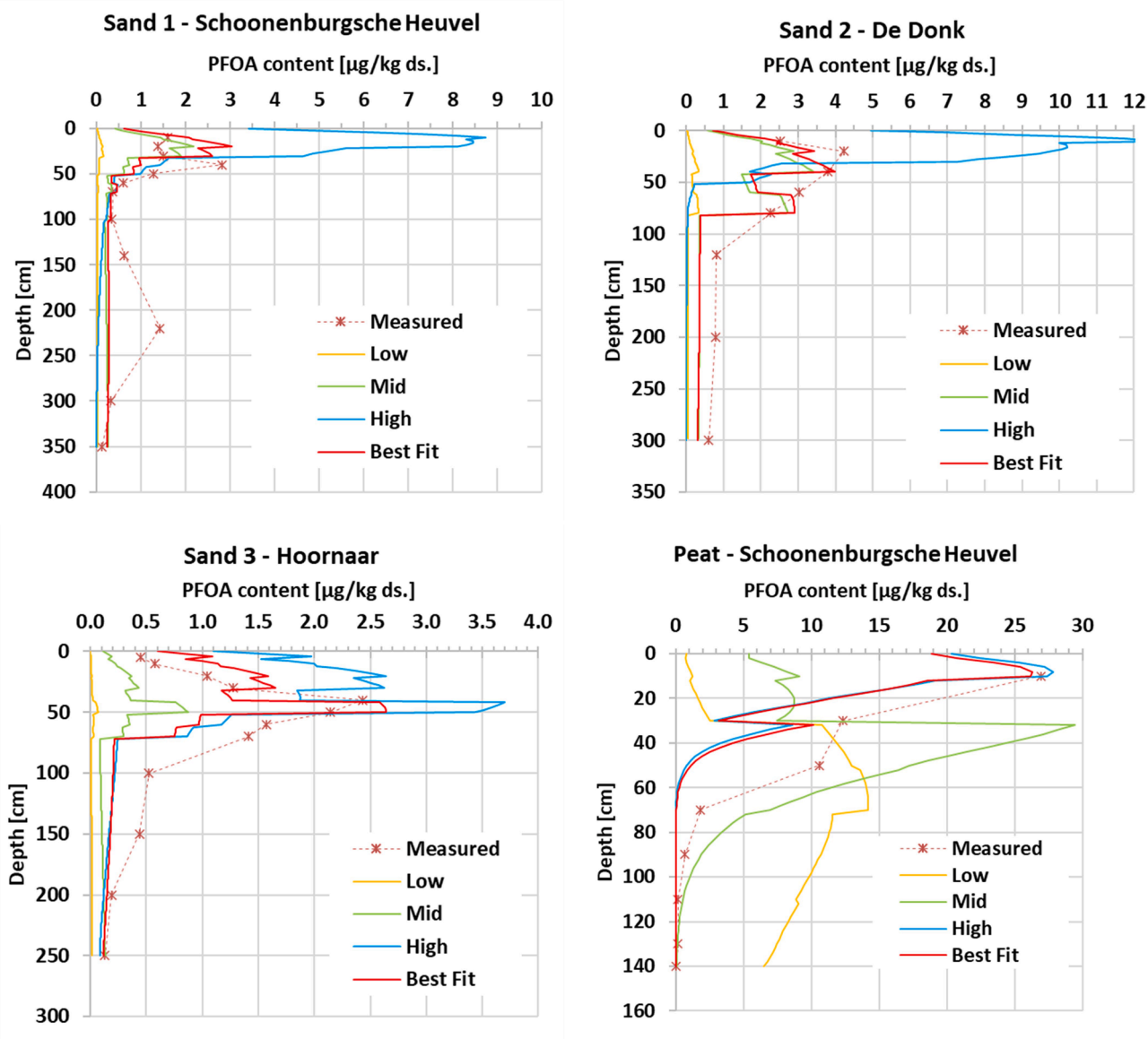

Fig. 2. Modelled versus observed depth plots of PFOA content for the four sampled soils.

contains about 20% OM at 10 and 30 cm-bs and about 60-75% OM at larger depths. The upper two samples consist of loam and silty loam having a median grain size of 37 and 19 μm; peat is present below. The TGA weight loss in the range 450-550°C is also higher with 3.18 - 5.03% for the peat samples and 1.5% for the two silt samples. However, no correlation with the weight loss at 110-450°C is indicated. The OC content according to the CS elemental analyser shows similar patterns as the OM content (except one low outlier at 90 cm-bs in Peat that showed 15% OC versus 62% OM). Linear regression based on all samples except the outlier sample indicates that the OM to OC ratio lies around 1.62 (where R^2 was 0.994).

PFAS contamination

The results of the analysis of all 18 PFAS compounds are provided in the Supporting Information. For PFOA and PFOS the results are plotted in Figs. 2 and 3, respectively. PFOA and PFOS were generally the PFAS compounds that were present in the highest contents in the topsoils. Other perfluorocarboxylic acids, outside of the scope of this study, were detected in lower contents (Supporting Information), with the exception of perfluorobutanoic acid (PFBA) in the topsoil of Sand 3 (Supporting Information).

For the sand soils, peak values of PFOA of 2.43 – 4.2 μg/kg are found several tens of centimeters below the surface (Fig. 2). A sorption front is observed below to appr. 100 cm-bs and low to intermediate concentrations are found down to the end of the soil profile sampled. The peak values lie above the national background value of 1.9 μg/kg, likely as result of the closeness of the sampling locations to the factory. The peak values at depth and continuous presence down to several meters depth indicate that PFOA is mobile in these soils and the highest atmospheric deposition has passed. PFOS shows different patterns in the sand soils, with highest content in the shallowest samples for Sand 1 and 3 and at 20 cm-bs for Sand 2, lower maximum contents of 0.64 – 1.1 μg/kg and values below detection limit deeper than 50 – 80 cm-bs (Fig. 3). The maximum contents lie below the national background value of 1.4 μg/kg.

The PFOA and PFOS contents are notably different for Peat with highest contents of 27 and 6.8 μg/kg, respectively, in the shallowest sample (Fig. 2). The contents drop strongly within a meter to values below detection limit for both compounds. The PFAS contents at shallow depth lie far above the national background values.

The depth-integrated amounts present were calculated for both

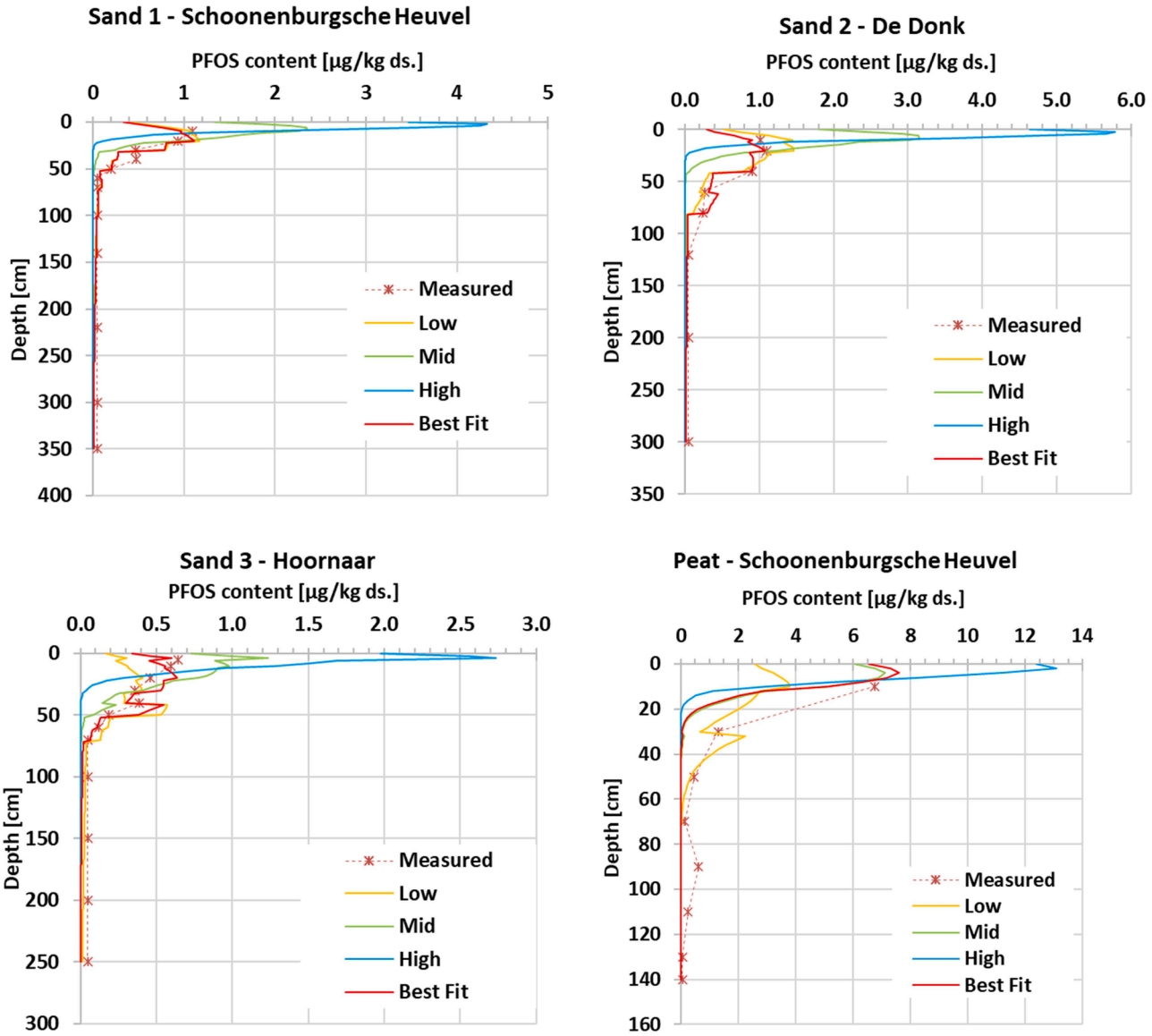

Fig. 3. Modelled versus observed depth plots of PFOS content for the four sampled soils.

Table 5
Depth-integrated amounts of PFAS present in the four soils sampled with the distance (rounded to whole kilometres) and compass direction from the fluoropolymers factory.

Location	Distance to factory (km)	Compass direction	PFOA (μg/m^2)	PFOS (μg/m^2)	PFOA to PFOS ratio
Sand 1	8	N	4454	749	5.9
Sand 2	9	NNE	6486	967	6.7
Sand 3	16	ENE	2523	492	5.1
Peat	8	N	4542	728	6.2

compounds at the four sites by integrating the contents across the depth (Table 5). The sites Sand 1 and Peat are adjacent to each other and show almost identical amounts. Both contents at Sand 2 are somewhat higher than these values whereas they are somewhat lower at Sand 3. The lowest amounts at Sand 3 are explained by the larger distance and stronger deviation from the dominant wind direction in the Netherlands, which is towards northeastern. The PFOA to PFOS ratios also vary somewhat among the soils sampled where the ratio is lowest at Sand 3 which is farthest away from the factory and highest at Sand 2 which lies most in the prominent wind direction from the factory. This may suggest that the influence of the factory is more clearly expressed at Sand 2, while other sources of PFAS play a larger role for Sand 3.

Transport modelling

The model results in terms of concentration-depths plots for the year 2020 are presented in Figs. 2 and 3 for the three different K_{oc} values as well as the best fit. The following observations are made for PFOA: 1. the depths of the highest content ("peaks") can be well reproduced for Sand 2 and 3, slightly less for Sand 1, and also for Peat with high K_{oc}. 2. For the sand soils, the scenario based on low K_{oc} strongly underestimates the contents, the scenario with middle K_{oc} value closely matches the profiles of Sand 1 and 2, this value underestimates the profile of Sand 3 while the high K_{oc} is too high. 3. The decrease in PFOA under the peak value tends to be sharper in the model for the optimum fits than in reality especially for Sand 3 and Peat. 4. PFOA contents of 0.5 μg/kg or higher below 100 cm-bs are not described by the model.

For PFOS, the following is noted: 1. literature values of K_{oc} are higher for PFOS than for PFOA, so the sorption affinity is higher. Indeed, the maximum contents are at shallower depth for the sand soils for both the observations and the model results. 2. The model scenarios based on middle and high K_{oc} values overestimate the sorption at shallow depth in the three sand soils. The observed profiles are closer to the modelled ones with low K_{oc}. The best fits have K_{oc} values close to the low values and can reproduce the reaction fronts below the maximum contents well. 3. The sampling density of the peat soil was too low at shallow depth for a meaningful comparison of the models and the observations. The model scenario based on middle or low K_{oc} value matches closer than that based on the high K_{oc} value.

Table 6 summarizes the log K_{oc} values for the best fits. The optimum value for PFOS in Sand 2 is low compared to the likely range (cf. Table 3). The other values lie within 1 standard deviation from the mean. For Peat, one should note that this soil contains two different horizons: an upper mineralogical horizon with OM associated with it and an organic horizon below. The assumption of a single K_{oc} for both horizons is a gross simplification but no attempt was made to optimise the modelling. The three sand soils have a similar geological setting and the difference in log K_{oc} is about 0.3 for both PFOA and PFOS, which means that the sorption intensity varies a factor of 2 among the three soils. Additional data fitting is of little interest.

Table 6
Log K_{oc} values for the best fits to the individual content-depths profiles.

Compound	Sand 1	Sand 2	Sand 3	Peat
PFOA	2.38	2.34	2.62	2.76
PFOS	2.71	2.55	2.86	3.14

The best fit values were used to investigate the expected propagation of the PFAS contamination through the soils over time, by extending the model calculations another 50 years until 2070. The result is expressed as the ratio between the modelled mass present in a soil profile as a function of time divided by the total mass deposited in 1970-2012 (which was set equal to the depth-integrated amount present in 2020; cf. Table 5). Fig. 4 presents the results for PFOA and PFOS. The curves for the three sand soils are very similar due to small differences in K_d. The result for PFOA suggests that some mass has already leached out of the sand soils in 2020, which would imply that the depth-integrated amount present does not exactly match the modelled amount present. We did not correct for this to avoid over-fitting. The total mass present gradually declines and 10-20% is still left in the soil at 2070. The situation is entirely different for Peat where all mass remains within the soil until to 2070. This also holds for PFOS. However, the retention of PFOS is stronger than of PFOA due to the higher K_{oc} so almost no mass was leached from the sand soil in 2020 and more than 50% is still present in these soils in 2070. This illustrates how a single, historical PFAS contamination becomes split in time into a PFOA groundwater contamination and a PFOS soil contamination.

Discussion

Soil contamination and historical PFAS deposition

PFOA

The PFOA contents are clearly higher than the PFOS contents in the measured profiles, consistent with PFOA being the dominant PFAS component in the historical emissions from the factory (Koch et al., 2017; Zeilmaker et al., 2016; Expertisecentrum PFAS, 2018c). The amounts of both PFOA and PFOS present are similar for adjacent Sand 1 and Peat (Table 5), confirming the assumption that these soils have been exposed to a similar atmospheric deposition. The maximum PFOA contents in the sand soils lie above the national background value of 1.9 μg/kg whereas those of PFOS lie below the national background value of 1.4 μg/kg. The absence of other nearby sources is a strong indication that the sampled sites were subject to additional atmospheric deposition of PFOA from the nearby factory. The contents in the top of Peat are considerably higher due to a much stronger retardation.

The maximum PFOA contents were found at depths of 20-50 cm below ground level in the three sand soils. Since we sampled undisturbed soils, these maxima must be the result of the slow transport of PFOA downward in these soils. The observation that peak contents are found at some depth below surface is also a direct indication that deposition of PFOA has become less or stopped, consistent with the phasing out of the use of PFOA at the factory in 2012. PFOA has been transported downward in the soil since that time, reducing the PFOA content at the surface. The OM/OC content in the sand soils is the highest in the top layer and decreases with increasing depth. So the sorption capacity for PFAS is also highest in the top layer because the sand soils are rather unreactive at larger depths. The samples were taken in October 2020, 8 years after the phasing out. It also implies that the transport rate of PFAS will be higher at larger depths.

The HYDRUS simulations support these findings as the model results show generally adequate simulated depth profiles based on general parameters combined with K_{oc} as fitted parameter that falls in the literature range (most notably Nguyen et al., 2020). The modelled maximum contents coincide with the measured ones so the downward transport of PFOA can be well captured. Upon result, the combination of measurements and simulations allowed us to establish a plausible reconstruction of soil transport of PFOA due to the historical emission from the factory and related atmospheric deposition. Here, limited data was available on the emission history from the factory in the initial period 1970-1990, so the emission based concentration scenario in the

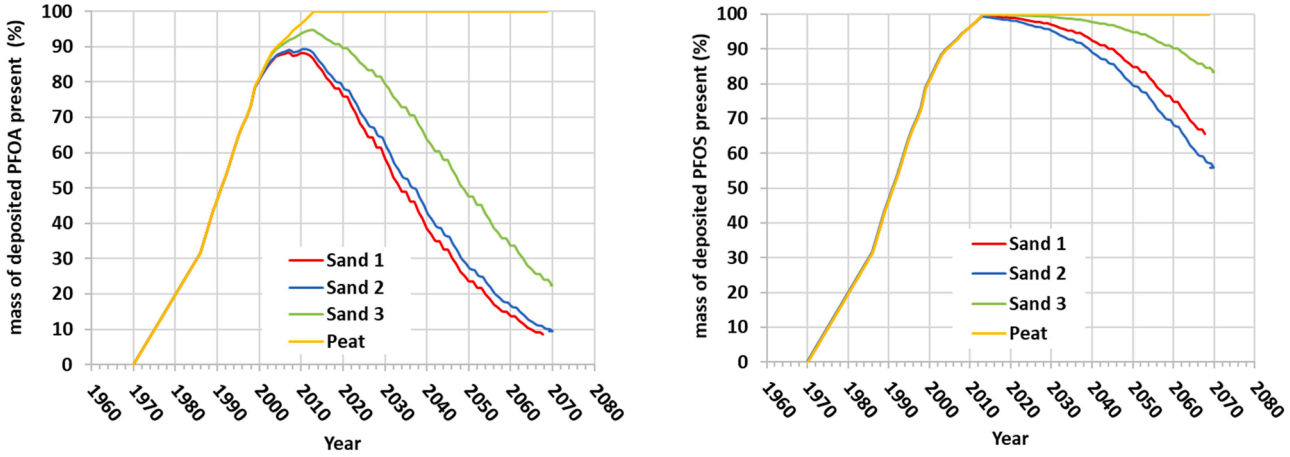

Fig. 4. Propagation of the total mass of PFAS deposited through the soils in time.

period 1970-1990 is subject to uncertainty. It seems that the temporal variation in emission and associated deposition becomes averaged in the soil profiles with effects of heterogeneity in soil properties, and sampling and analytical accuracies.

PFOS

In the soils, the highest PFOS contents were found in the first or second sample from the surface. The shallower peak content is explained by the fact that PFOS adsorbs stronger to organic matter, hence the shallow penetration depth of PFOS. The depth profiles of PFOS could be well modelled for the sand soils, where K_{oc} was fitted and the atmospheric deposition history from the factory was assumed. However, it is impossible that for the PFOS contamination levels observed PFOS originates from the factory in the same way as PFOA does. Another major source having a comparable release history must have been present. In first instance, one may assume waste incinerators as source for diffuse contamination of PFOS and also other PFAS compounds, including PFOA. The total amount of waste incinerated has increased in the Netherlands from 325 kton in 1970 via 2270 kton in 1980, 2845 kton in 1990 to ~ 8000 kton/y since 2014 (CLO, 2021). The oldest and biggest incinerator is situated in Rotterdam harbour area (capacity 1300 kton/y in 2016), operational since 1973 (Rijkswaterstaat, 2017b) and 40-55 km away to the west from the sampled sites. Another incinerator is in Moerdijk, operational since 1982 (capacity 1200 kton/y) and 30-36 km away in soutwestern direction. A third smaller one (396 kton/y) is in Dordrecht near the PFAS factory, also operational since 1973 and 10-18 km away in southern to southwestern direction.

Since 1993, it is demanded in the Netherlands that the temperature in the incinerator is at least 850°C (Besluit Luchtemissies Afvalverbranding, 1993). Nowadays, the temperature is commonly ~1000°C and scrubbers are used to remove gaseous HF from the flue gases together with HCl and SO_2. Both PFOS and PFOA can be broken down with incineration where operating temperatures around 1000°C are found as optimal for PFAS destruction (Stoiber et al., 2020). Khan et al. (2020) computed that the PFOS half-life is less than 1 s during thermal decomposition above 750°C. Despite this, PFOS and also PFOA and other PFAS were observed in fly ashes and bottom ashes produced from the incineration of municipal solid waste where the operating temperature was not specified (Liu et al., 2021). Solo-Gabriele et al. (2020) observed an inverse relationship between total PFAS remaining in ash leachates and the incineration temperature between 800 and 950°C. This indicates that it is not self-evident that PFAS become completely decomposed in waste incinerators. It thus seems that Dutch waste incinerators can be a (historical) source for diffuse contamination of soils with PFOS (and other PFAS including PFOA) because these incinerators were not operating at sufficiently high temperature in the past and/or the time was too short for complete thermal decomposition. The latter may be partly due to the fact that the high temperature is not reached throughout the oven of the waste incinerator. The existence of "cold spots" in the oven is evidenced by the presence of considerable amounts of unburnt natural organic matter in the ashes (Meima et al., 1999; Ferrari et al., 2002; Van Zomeren et al., 2004, 2009).

PFAS retention mechanisms

The results from the HYDRUS simulations show that meaningful depth profiles for PFOA and PFAS can be obtained for the sand soils using default parameters for the soil properties where linear sorption is the only retention process. A simple, classical model concept was thus sufficient to model transport of PFAS in these soils under annually averaged infiltration conditions. For the soil contents observed for PFOA and the best-fit K_{oc} values, the pore water concentrations of PFOA are 300 - 400 ng/L at most (or 0.75 - 1 nmol/L) which is far below the solubility of PFOA in water being 9500 mg/L (EPA, 2017). The same holds for PFOS for which the solubility is 680 mg/L. It is inevitable that partitioning to soil organic matter and adsorption at the AWI play important roles as retention mechanisms in the sand soils. The distribution coefficients employed take into account both and not only partitioning to soil organic matter although they were based on K_{oc} values. This was allowed by the linear nature of AWI adsorption at the low PFAS concentrations and the steady-state conditions assumed for the soil physics.

Metal oxides and clay minerals may play a role in sorption of PFAS (e.g. Li et al. 2018, Campos-Pereira et al. 2020). Their specific binding capacity is lower than for soil organic carbon. Wang et al. (2021) established for PFOS specific distribution coefficients of 568, 19 and 7 cm^3/g for organic carbon, clay+silt and metal oxides, respectively. Values of 3.47 for PFOS and 1.66 for PFOA can be deduced from Fabregat-Palau et al. (2021) for the specific distribution coefficient of clay+silt. Combining the soil characteristics and these values, it is justified to assume that sorption to organic matter is dominant in the upper part of our sand soils (cf. Higgins and Luthy 2006, Milinovic et al. 2015). The organic matter content is below 0.4% in the part below 0.5-1 m depth of these soils while the clay and silt contents are negligible. The bleached color of the deeper sediment indicates lack of oxides. The sorption coefficient of this stretch is thus very low and might still be controlled by organic matter. We also selected these soils on purpose for their low reactivity in order to reconstruct the deposition history of PFAS in the investigated area. Adsorption at the AWI is likely the most important retention mechanism in this stretch.

Sorption in the peat soil was also modelled using the same K_{oc} concept. However, this is probably a simplification as pH-dependent

sorption to humic and fulvic acids in combination with effects of cations present is likely, in addition to hydrophobic sorption to humin (Campos Pereira et al., 2018). This holds more for PFOA than for PFOS. The clastic component majorly consists of clay and silt which possess retention capacity too. Note that accurate modelling of PFAS transport in this soil lies beyond the scope of this manuscript. The peat soil was primarily sampled to investigate whether similar total amounts were observed as in the adjacent sand soil, which indeed was true.

Conclusions

For the first time, detailed concentration-depth profiles of PFOA and PFOS were measured in undisturbed soils s downwind from a fluoropolymer factory that emitted PFOA. Three sand soils show similar patterns with maximum contents several tens of centimeters below the surface, prominent sorption in the top soil and low contents in the vadose zone down to several meters. This confirms the hypothesis that the vertical variation of PFOA content in undisturbed sand soils in the common downwind direction from the factory reflects the historical atmospheric deposition of PFOA from that factory. An adjacent peat-rich soil contained the same depth-integrated amount but considerably higher contents at shallower depth and less downward penetration. This illustrates large differences in retention causing highly variable PFOA soil contents while the contamination source is identical. The peak values at depth and continuous presence down to several meters depth indicate that PFOA is mobile in these soils and the highest atmospheric deposition has passed.

Less PFOS is detected in the soils and PFOS has not migrated as deep as PFOA. The shallower infiltration depths of PFOS confirm its stronger sorption. The different ratios of the total amount of PFOA to that of PFOS suggest another, major source for PFOS aside from the PFAS factory. Possibly, the diffuse PFOS contamination originates from waste incinerators where two large ones have been present in the most common upwind direction from the sites studied. Additional research is needed to confirm or falsify this explanation.

The depth profiles in the sand soils can be adequately modelled with linear retention using a plausible value for the normalised organic carbon to water partition coefficient distribution coefficient, the most plausible explanation for the deposition history and standard properties of the soil matrix. Actually, the linear retention observed will also include adsorption at the air-water interface under low PFAS concentrations, while additional physico-chemical processes may be neglected under the conditions found. Based on the best-fit model scenarios, PFAS contents are projected to decrease in the topsoil as a result of gradual transport to groundwater on a time scale of decades. Supported by measurements and modelling, this study illustrates that PFOA, and to a lesser extent PFOS, should not be treated as immobile contaminants in topsoil as is currently the case in Dutch soil policy, but rather as mobile contaminants of which the legacy amounts in soil will pollute groundwater for many decades.

CRediT authorship contribution statement

TG did the field and lab work, the data interpretation including the modelling. JD and JG initiated the project, supported the field work, did the data interpretation and model conceptualisation. TG, JD and JG selected the field sites. HB did the lab work. ARD did the field and lab work. TG and JG did the writing and the others commented on the writing.

Declaration of Competing Interest

The authors declare that they have no known competing financial interests or personal relationships that could have appeared to influence the work reported in this paper.

Data availability

The data will be made available via the database website of TNO Geological Survey of the Netherlands.

Acknowledgments

This article is an elaboration of the thesis of TG in fulfillment of the MSc- degree at Utrecht University, conducted at TNO under the supervision of JG and JD. We thank Noémi Brunschwiler for performing additional HYDRUS calculations. This project was financed by TNO under the roadmap Geological Survey of the Netherlands and is associated with the national Topsector Water program. Data from this study will be made publicly available through the data and information system (DINO) of TNO Geological Survey of the Netherlands (www.dinoloket.nl).

Supplementary materials

Supplementary material associated with this article can be found, in the online version, at doi:10.1016/j.envadv.2022.100332.

References

Agilent Technologies (2017). Recommended plumbing configurations for reduction in per/polyfluoroalkyl substance background with agilent 1260/1290 infinity (II) LC systems. https://www.agilent.com/cs/library/applications/5991-7863EN.pdf (accessed 05-12-2022).

Besluit Luchtemissies Afvalverbranding (1993). Besluit van 7 januari 1993 houdende voorschriften ter voorkoming en vermindering van luchtverontreiniging veroorzaakt voor de verbranding van afvalstoffen.

Brandsma, S.H., Koekkoek, J.C., van Velzen, M.J.M., de Boer, J., 2019. The PFOA substitute GenX detected in the environment near a fluoropolymer manufacturing plant in the Netherlands. Chemosphere 220, 493–500.

Brusseau, M.L., 2018. Assessing the potential contributions of additional retention processes to PFAS retardation in the subsurface. Sci. Total Environ. 613–614, 176–185.

Buck, R.C., Franklin, J., Berger, U., Conder, J.M., Cousins, I.T., De Voogt, P., van Leeuwen, S.P., 2011. Perfluoroalkyl and polyfluoroalkyl substances in the environment: terminology, classification, and origins. Integr. Environ. Assess. Manag. 7, 513–541.

Campos Pereira, H., Ullberg, M., Kleja, D.B., Gustafsson, J.P., Ahrens, L, 2018. Sorption of perfluoroalkyl substances (PFASs) to an organic soil horizon - effect of cation composition and pH. Chemosphere 207, 183–191.

Campos-Pereira, H., Kleja, D.B., Sjostedt, C., Ahrens, L., Klysubun, W., Gustafsson, J.P., 2020. The adsorption of Per- and polyfluoroalkyl substances (PFASs) onto Ferrihydrite is governed by surface charge. Environ. Sci. Technol. 54, 15722–15730.

Carsel, R.F., Parrish, R.S., 1988. Developing joint probability distributions of soil water retention characteristics. Water Resour. Res. 24, 755–769.

Cordner, A., Goldenman, G., Birnbaum, L.S., Brown, P., Miller, M.F., Mueller, R., Patton, S., Salvatore, D.H., Trasande, L., 2021. The true cost of PFAS and the benefits of acting now. Environ. Sci. Technol. 55, 9630–9633. https://doi.org/10.1021/acs.est.1c03565.

CEU, 2019a. EU Action to Address Risks Related to PFAS - Information from the Danish, Luxembourg, Netherlands and Swedish Delegations. Council of the European Union note 15039/19, 11 December 2019.

CEU, 2019b. Towards a Sustainable Chemicals Policy Strategy of the Union - Council conclusions. Council of the European Union outcome of proceedings 10713/19, 26 June 2019.

CLO (2021). Afvalverbrandingsinstallaties, aantal en capaciteit, 1970-2018. Published at www.clo.nl, 8 January 2021.

De Vries, F. (1999). Karakterisering van Nederlandse gronden naar fysisch-chemische kenmerken. DLO-Staring Centrum, report no. 654.

Du, Z., Deng, S., Bei, Y., Huang, Q., Wang, B., Huang, J., Yu, G., 2014. Adsorption behavior and mechanism of perfluorinated compounds on various adsorbents-a review. J. Hazard. Mater. 274, 443–454.

EFSA, 2020. Risk to human health related to the presence of perfluoroalkyl substances in food. EFSA J. 18 (9), 6223. /.

EPA, 2017. Technical Fact Sheet – Perfluorooctane Sulfonate (PFOS) and Perfluorooctanoic Acid (PFOA). United States Environmental Protection Agency, p. 8. EPA 505-F-17-001, November 2017.

Eschauzier, C., Raat, K.J., Stuyfzand, P.J., De Voogt, P., 2013. Perfluorinated alkylated acids in groundwater and drinking water: identification, origin and mobility. Sci. Total Environ. 458-460, 477–485.

Expertisecentrum PFAS (2017). Luchtdepositie onderzoek PFOA en HFPO-DA (GenX) Dordrecht en omgeving. Expertisecentrum PFAS, report no. 20DDT221-1.17.

Expertisecentrum PFAS (2018a). Aanvullend luchtdepositie onderzoek PFOA en HFPO-DA (GenX) Dordrecht en omgeving. Expertisecentrum PFAS, report no. C05044.000229.0100/079794902 A.
Expertisecentrum PFAS (2018b). Poly- en PerFluor Alkyl Stoffen (PFAS). Kennisdocument over stofeigenschappen, gebruik, toxicologie, onderzoek en sanering van PFAS in grond en grondwater. Expertisecentrum PFAS, report no. DDT219-1/18-009.764.
Expertisecentrum PFAS (2018c). Aanwezigheid van PFAS in Nederland. Deelrapport B - Onderzoek van PFAS op potentiële risicolocaties. Expertisecentrum PFAS, report no. DDT219-1/18-008.228.
Expertisecentrum PFAS, VVMA, VKB, 2020. Guideline PFAS sampling (Handreiking PFAS bemonsteren), version 1.0, 25-06-2020.
Fabregat-Palau, J., Vidal, M., Rigol, A., 2021. Modelling the sorption behaviour of perfluoroalkyl carboxylates and perfluoroalkane sulfonates in soils. Sci. Total Environ. 801, 149343.
Ferrari, S., Belevi, H., Baccini, P., 2002. Chemical speciation of carbon in municipal solid waste incinerator residues. Waste Manag. 22, 303–314.
Gebbink, W.A., Van Leeuwen, S.P.J., 2020. Environmental contamination and human exposure to PFASs near a fluorochemical production plant: review of historic and current PFOA and GenX contamination in the Netherlands. Environ. Int. 137, 105583.
Ghisi, R., Vamerali, T., Manzetti, S., 2019. Accumulation of perfluorinated alkyl substances (PFAS) in agricultural plants: a review. Environ. Res. 169, 326–341.
Glüge, J., Scheringer, M., Cousins, I.T., Dewitt, J.C., Goldenman, G., Herzke, D., Lohmann, R., Ng, C.A., Trier, X., Wang, Z., 2020. An overview of the uses of per- and polyfluoroalkyl substances (PFAS). Environ. Sci. Process. Impacts 22, 2345–2373. https://doi.org/10.1039/d0em00291g.
Guo, B., Zeng, J., Brusseau, M.L., 2020. A mathematical model for the release, transport, and retention of per- and polyfluoroalkyl substances (PFAS) in the Vadose Zone. Water Resour. Res. 57, e2019WR026667.
Herrick, R.L., Buckholz, J., Biro, F.M., Calafat, A.M., Ye, X, Xie, C., Pinney, S.M., 2017. Polyfluoroalkyl substance exposure in the Mid-Ohio River Valley, 1991-2012. Environ. Pollut. 228, 50–60.
Higgins, C.P., Luthy, R.G., 2006. Sorption of perfluorinated surfactants on sediments. Environ. Sci. Technol. 40 (23), 7251–7256.
Joerss, H., Apel, C., Ebinghaus, R., 2019. Emerging per- and polyfluoroalkyl substances (PFASs) in surface water and sediment of the North and Baltic Seas. Sci. Total Environ. 686, 360–369.
Kasozi, G.N., Nkedi-Kizza, P., Harris, W.G., 2009. Varied carbon content of organic matter in histosols, spodosols and carbonatic soils. Soil Sci. Soc. Am. J. 73, 1313–1318.
Khan, M.Y., So, S., Da Silva, G., 2020. Decomposition kinetics of perfluorinated sulfonic acids. Chemosphere (238), 124615.
Koch, W.W.R., Droge R. & Coenen, P.W.H.G. (2017). Archiefonderzoek historische emissies DuPont Dordrecht. TNO report no. TNO 2016 R11743.
Lath, S., Knight, E.R., Navarro, D.A., Kookana, R.S., McLaughlin, M.J., 2019. Sorption of PFOA onto different laboratory materials: filter membranes and centrifuge tubes. Chemosphere 222, 671–678.
Li, Y., Oliver, D.P., Kookana, R.S., 2018. A critical analysis of published data to discern the role of soil and sediment properties in determining sorption of per and polyfluoroalkyl substances (PFASs). Sci. Total Environ. 628-629, 110–120.
Li, F., Duan, J., Tian, S., Ji, H., Zhu, Y., Wei, Z., Zhao, D., 2020. Short-chain per- and polyfluoroalkyl substances in aquatic systems: occurrence, impacts and treatment. Chem. Eng. J. 380, 122506.
Liu, S., Zhao, S., Liang, Z., Wang, F., Sun, F., Chen, D., 2021. Perfluoroalkyl substances (PFASs) in leachate, fly ash, and bottom ash from waste incineration plants: Implications for the environmental release of PFAS. Sci. Total Environ. 795, 148468.
Ma, D., Zhong, H., Lv, J., Wang, Y., Jiang, G., 2022. Levels, distributions, and sources of legacy and novel per- and perfluoroalkyl substances (PFAS) in the topsoil of Tianjin, China. J. Environ. Sci. 112, 71–81.
Meima, J.A., Van Zomeren, A., Comans, R.N.J., 1999. Complexation of Cu with dissolved organic carbon in municipal solid waste incinerator bottom ash leachates. Environ. Sci. Technol. (33), 1424–1429.
Milinovic, J., Lacorte, S., Vidal, M., Rigol, A., 2015. Sorption behaviour of perfluoroalkyl substances in soils. Sci. Total Environ. 511, 63–71.
NEN - Netherlands Committee for Standardization (2018). NEN 7779: Environment, food and feed - Measurement uncertainty (Dutch Language).
Newell, C.J., Adamson, D.T., Kulkarni, P.R., Nzeribe, B.N., Connor, J.A., Popovic, J., Stroo, H.F., 2021. Monitored natural attenuation to manage PFAS impacts to groundwater: potential guidelines. Remediation 2021, 1–11.
Nguyen, T.M.H., Bräunig, J., Thompson, K., Thompson, J., Kabiri, S., Navarro, D.A., Kookana, R.S., Grimison, C., Barnes, C.M., Higgins, C.P., McLaughlin, M.J., Mueller, J.F., 2020. Influences of chemical properties, soil properties, and solution ph on soil–water partitioning coefficients of per-and polyfluoroalkyl substances (PFASs). Environ. Sci. Technol. 54, 15883–15892.
Prevedouros, K., Cousins, I.T., Buck, R.C., Korzeniowski, S.H., 2006. Sources, fate and transport of Perfluorocarboxylates – a critical review. Environ. Sci. Technol. 40, 32–44.
RIVM, 2020. Achtergrondwaarden Perfluoralkylstoffen (PFAS) in de Nederlandse Bodem. Rijksinstituut voor Volksgezondheid en Milieu, p. 56 briefrapport 2020-0100.
RIVM, 2021. Analyse Bijdrage Drinkwater en Voedsel Aan Blootstelling EFSA-4 PFAS in Nederland en Advies Drinkwaterrichtwaarde. Rijksinstituut voor Volksgezondheid en Milieu project no. M/270071, date 03-05-2021.
Roskam, G., Klaver, G. & Griffioen, J. (2008). Methodeontwikkeling voor het bepalen van het gehalte reactief ijzer. TNO/Deltares, report no. 2008-U-R1288/A.
Rijkswaterstaat, 2017a. Resultaten Meetprogramma FRD en PFOA Stoffen Rondom Chemours te Dordrecht. Rijkswaterstaat, p. 31 report no. RWS-2017/24775, 13 June 2017.
Rijkswaterstaat, 2017b. Afvalverwerking in Nederland, Gegevens 2016. Rijkswaterstaat. November 2017, ISBN 978-94-91750-18-2.
Rijkswaterstaat, 2020. Bronnen van PFAS Voor Het Nederlandse Oppervlaktewater. Rijkswaterstaat, p. 49 report, 14 July 2020.
Schaap, M.G., Leij, F.J., van Genuchten, M.Th, 2001. Rosetta: a computer program for estimating soil hydraulic parameters with hierarchical pedotransfer functions. J. Hydrol. 251, 163–176.
Schulz, K., Silva, M.R., Klaper, R., 2020. Distribution and effects of branched versus linear isomers of PFOA, PFOS, and PFHxS: a review of recent literature. Sci. Total Environ. 733, 139186.
Silva, J.A.K., Šimůnek, J., McCray, J.E., 2020. A modified HYDRUS model for simulating PFAS transport in the Vadose Zone. Water 12, 2758.
Silva, J.A.K., Martin, W.A., McCray, J.E., 2021. Air-water interfacial adsorption coefficients for PFAS when present as a multi-component mixture. J. Contam. Hydrol. 236, 103731.
Šimůnek, J., Šejna, M., Saito, H., Sakai, M., van Genuchten, M.Th., 2008. The HYDRUS-1D Software Package for Simulating the Movement of Water, Heat, and Multiple Solutes in Variably Saturated Media, Version 4.08, HYDRUS Software Series 3. Department of Environmental Sciences, University of California Riverside, Riverside, California, USA, p. 330.
Solo-Gabriele, H.M., Jones, A.S., Lindstrom, A.B., Lang, J.R., 2020. Waste type, incineration, and aeration are associated with per- and polyfluoroalkyl levels in landfill leachates. Waste Manag. 107, 191–200.
Stoiber, T., Evans, S., Naidenko, O.V., 2020. Disposal of products and materials containing per- and polyfluoroalkyl substances (PFAS): a cyclical problem. Chemosphere 260, 127659.
USDA (1987). Soil mechanics level I. Module 3 USDA textural soil classification. Study Guide. United States Department of Agriculture, 48 pp.
van Genuchten, M.Th., 1980. A closed-form equation for predicting the hydraulic conductivity of unsaturated soils. Soil Sci. Soc. Am. J. 44, 892–898.
Van Zomeren, A., Comans, R.N.J., 2004. Contribution of natural organic matter to copper leaching from municipal solid waste incinerator bottom ash. Environ. Sci. Technol. 38, 3927–3932.
Van Zomeren, A., Comans, R.N.J., 2009. Carbon speciation in municipal solid waste incinerator (MSWI) bottom ash in relation to facilitated metal leaching. Waste Manag. 29, 2059–2064.
Vecitis, C.D., Park, H., Cheng, J., Mader, B.T., Hoffmann, M.R., 2008. Enhancement of Perfluorooctanoate and Perfluorooctanesulfonate Activity at Acoustic Cavitation Bubble Interfaces. J. Phys. Chem. 112, 16850–16857.
Wang, Z., MacLeod, M., Cousins, I.T., Scheringer, M., Hungerbühler, K., 2011. Using COSMOtherm to predict physicochemical properties of poly- and perfluorinated alkyl substances (PFASs). Environ. Chem. 8, 389–398.
Wang, W., Rhodes, G., Ge, J., Yu, X., Li, H., 2020. Uptake and accumulation of per- and polyfluoroalkyl substances in plants. Chemosphere (261), 127584.
Wang, Y., Khan, N., Huang, D., Carroll, K.C., Brusseau, M.L., 2021. Transport of PFOS in aquifer sediment: transport behavior and a distributed-sorption model. Sci. Total Environ. 779, 146444.
Zafeiraki, E., Costopoulou, D., Vassiliadou, I., Leondiadis, L., Dassenakis, E., Traag, W., Hoogenboom, R.L.A.P., Van Leeuwen, S.P.J., 2015. Determination of perfluoroalkylated substances (PFASs) in drinking water from the Netherlands and Greece. Food Addit. Contam. Part A (32), 2048–2057.
Zareitalabad, P., Siemens, J., Hamer, M., Amelung, W., 2013. Perfluorooctanoic acid (PFOA) and perfluorooctanesulfonic acid (PFOS) in surface waters, sediments, soils and wastewater – a review on concentrations and distribution coefficients. Chemosphere 91 (6), 725–732.
Zeilmaker, M.J., Janssen, P., Versteegh, A., Van Pul, A., De Vries, W., Bokkers, B., Wuijts, S., Oomen, A. & Herremans, J. (2016). Risicoschatting emissie PFOA voor omwonenden. Locatie: DuPont/Chemours, Dordrecht, Nederland. RIVM Briefrapport 2016-0049.
Zeng, J., Guo, B., 2021. Multidimensional simulation of PFAS transport and leaching in the vadose zone: impact of surfactant-induced flow and subsurface heterogeneities. Adv. Water Resour. 155, 104015.
Zenobio, J.E., Salawu, O.A., Han, Z., Adeleye, A.S., 2022. Adsorption of per- and polyfluoroalkyl substances (PFAS) to containers. J. Hazard. Mater. Adv. 7, 100130.
Zhang, D.Q., Zhang, W.L., Liang, Y.N., 2019. Adsorption of perfluoroalkyl and polyfluoroalkyl substances (PFASs) from aqueous solution - a review. Sci. Total Environ. 694, 133606.
Zhou, D., Brusseau, M.L., Zhang, Y., Li, S, Wei, W, Sun, H.G., Zheng, C., 2021. Simulating PFAS adsorption kinetics, adsorption isotherms, and nonideal transport in saturated soil with tempered one-sided stable density (TOSD) based models. J. Hazard. Mater. 411, 125169.